



Electrical characterization of rare-earth implanted GaN

P.J. Janse van Rensburg^{a,*}, F.D. Auret^a, V.S. Matias^b, A. Vantomme^b

^a Department of Physics, University of Pretoria, Pretoria 0002, South Africa

^b Instituut voor Kern-en Stralingsfysica and INPAC, KULeuven, 3001 Leuven, Belgium

ARTICLE INFO

PACS:

78.66.Fd

91.60.Ed

68.55.Ln

61.72.Vv

Keywords:

GaN

Implantation

Rare-earth

Defects

ABSTRACT

Deep-level transient spectroscopy (DLTS) measurements were used to characterize the electrical properties of MOCVD grown, europium- (Eu) and xenon- (Xe) implanted GaN films on sapphire substrates. Implantation energy was 80 keV with a fluence of $1 \times 10^{14} \text{ cm}^{-2}$ along a channeled crystallographic direction. Defect levels were observed at $E_c - 0.19 \text{ eV}$ for both Eu- and Xe-implantation which were predicted to be a rare-earth related donor level by theoretical calculations. Other defect levels are observed with energy levels located at 0.22, 0.68, 0.49, 0.60, 0.77 eV and 0.48, 0.64, 0.45, 0.72 eV below the conduction band for Eu and Xe implantation, respectively. Some of these levels have similar defect signatures and can be related to other implantation related defects introduced in erbium, praseodymium and helium implantations.

© 2009 Elsevier B.V. All rights reserved.

1. Introduction

GaN is a material that has received a lot of attention for its potential use for optoelectronic applications such as light emitting diodes, detectors and laser diodes [1]. As a consequence of its wide (3.4 eV) direct band-gap, GaN demonstrates low thermal carrier generation rates and lower luminescence thermal quenching when compared to Si, for example. Furthermore, GaN demonstrates higher radiation hardness, compared to Si or GaAs. These properties make GaN a suitable host for optical dopants introduced by ion implantation.

Rare-earth (RE) elements have already been used in optoelectronic devices, such as the Nd:YAG laser, YBr:Eu phosphors or Er in optical fibers [2]. These elements have partially filled inner 4f electron shells shielded by completely filled outer 5s and 5p shells. Intra 4f electronic transitions result in very sharp optical emission at wavelengths ranging from ultraviolet to infrared covering the visible spectrum. The wavelength of the emitted light is almost independent of the host material. However, the host determines radiative transition probabilities and thereby plays an important role on the luminescence output.

Red, green and blue luminescence have been demonstrated [3] by doping GaN with europium (Eu), erbium (Er) and thulium (Tm), respectively. However, the exact mechanisms responsible for RE 4f electrons excitation and optical emission in GaN remain

incompletely understood, and described through models derived from theoretical calculations [4].

It is believed that RE ions will induce a donor level in the band gap of GaN, which will be involved in the formation of an exciton trap. The exciton recombination is non-radiative but is thought to excite the RE f-shell through an Auger mechanism. In fact, Filhol et al. [5] have calculated that Eu, Er and Tm will introduce donor levels at 0.2 eV below the conduction band.

Up to now, very little experimental work has been performed to show the existence of such a donor level. Song et al. reported that implantation of Er and Pr induce donor levels at 0.188 and 0.190 eV [6] below the conduction band of GaN, respectively. However, with this work we also observe similar levels after Xe implantation, leading to the conclusion that the reported levels are due to implantation induced damage. Xe is expected to be chemically inert and have a size and mass very similar to the RE ions used, and should therefore generate the same implantation damage profile.

2. Experimental

We have implanted MOCVD grown n-type GaN thin films at 80 keV with Eu and Xe ions at a fluence of $1 \times 10^{14} \text{ cm}^{-2}$. Implantations occurred with substrates at room temperature and aligning the incoming ion beam with the GaN $\langle 0001 \rangle$ crystalline axis. It was shown by means of RBS and HRXRD [7] that channelled implantation drastically reduces implantation damage.

* Corresponding author. Tel.: +27 12 420 2684; fax: +27 12 362 5288.
E-mail address: jvr@up.ac.za (P.J. Janse van Rensburg).

After implantation, samples were annealed at 900 °C under N₂ constant flow for 30 min. Before contact fabrication, the samples were degreased by boiling in trichloroethylene followed by rinsing in boiling isopropanol and thereafter in de-ionized water. The samples were then boiled for 3 min in aqua-regia and then rinsed in de-ionized water three times in an ultrasonic bath. Finally, the samples were etched in a HCl:H₂O (1:1) solution for 10 s. After cleaning, a layered ohmic contact structure consisting of Ti/Al/Ni/Au (150 Å/2200 Å/400 Å/500 Å) were deposited using an electron-beam evaporation system and then annealed at 500 °C for 5 min in an argon atmosphere. Circular Au Schottky contacts, 0.6 mm in diameter and 1000 Å thick, were resistively deposited through a metal contact mask, as close as possible to the ohmic contact to minimize the diode series resistance. Room temperature current–voltage (*IV*) and capacitance–voltage (*CV*) measurements were used to assess the quality of the Schottky contacts. Diodes with the lowest series resistance were then analysed by deep-level transient spectroscopy (DLTS). The implantation related defects were characterized by using a conventional lock-in amplifier DLTS system. The energy level relative to the conduction band, E_C-E_T , and apparent capture cross section, σ_a , of the defects, the combination of which is referred to as its DLTS signature, were determined from the Arrhenius plot of T^2/e vs. $1/T$, where e is the defect emission rate at a temperature T . DLTS spectra were acquired with filling pulse width of $T_p=0.2$ ms, pulse delay time $T_D=0.3$ ms, quiescent reverse bias $V_R=-2$ V, filling pulse amplitude $V_p=2.2$ V and temperature scans ranging from 100 to 350 K were performed at several rate windows ranging from 2 to 5000 s⁻¹. Below 100 K carrier freeze-out started to occur, decreasing the reverse biased capacitance drastically. Careful investigation showed no DLTS signals to be observed at temperatures below 100 K.

3. Results and discussion

Fig. 1 depicts the DLTS spectra measured for a reference sample (curve a), as well as Eu and Xe implanted samples (curves b and c), respectively). For clarity, the spectra are offset with respect to each other. The reference sample contained two prominent defect peaks, labelled EO2 and EO5. The energy levels of EO2 and EO5 were determined as $E_C-0.27$ eV and $E_C-0.61$ eV, respectively. EO2 and EO5 have approximately the same signatures as the E1 and E2 defects observed by Hacke et al. in n-GaN grown by hydride

vapour epitaxy [8] as well as the EO2 and EO5 defects observed by Auret et al. in MOVPE grown GaN [9]. They attribute the presence of these trap levels to defects introduced during growth. Haase et al. have also observed these levels in n-type GaN implanted with nitrogen [10].

The DLTS spectra of GaN implanted with Xe and Eu ions (curves (b) and (c) in Fig. 1) show additional and different defect levels related to implantation damage compared to the reference sample. The spectra obtained after implantation show very broad peaks in the temperature range where measurements were performed, which complicates accurate defect identification in the material. The main factors influencing these spectra is a drastic increase in the series resistance and reverse leakage current observed after implantation. The implantation creates a highly resistive layer below the GaN surface increasing the series resistance. The reverse leakage current at a bias of 1 V of the reference sample was in the order of 10⁻⁷ A, which increased to the range 10⁻⁵–10⁻⁴ A for the implanted samples. This indicates a large increase in recombination current due to defect levels acting as recombination centres within the band gap of the material. An increase in reverse leakage current and series resistance affects the biasing of the bridge circuit of the capacitance meter resulting in the capacitance transients being affected. This might be the cause of the non-zero base line observed in the spectra and can also lead to broadening of the DLTS peaks. Another possibility for the broadened DLTS peaks might be the result of the superposition of DLTS signals of several close lying trap levels or a distribution of trap levels formed within the band gap. High-resolution Laplace DLTS was attempted to investigate the possibility of several close lying deep levels, but did not provide any consistent and reliable results. This was mainly due to an insufficient signal to noise ratio required for high-resolution DLTS, due to the effects described above. In our analysis of the DLTS peaks, only the peak positions without any attempt to deconvolute them were used. This might result in less accurate determination of the defect signatures indicated in the Arrhenius plot shown in Fig. 2. The energy levels and apparent capture cross sections of the defect levels observed are summarized in Table 1 indicated with an uncertainty of at most 10%.

The E_{Eu5} defect level observed in the Eu implanted spectrum is most probably the same as the EO5 defect level seen in the reference sample. This can be attributed to the close alignment of these two defect signatures in the Arrhenius plot and the corresponding energy level of $E_C-0.61$ eV and capture cross

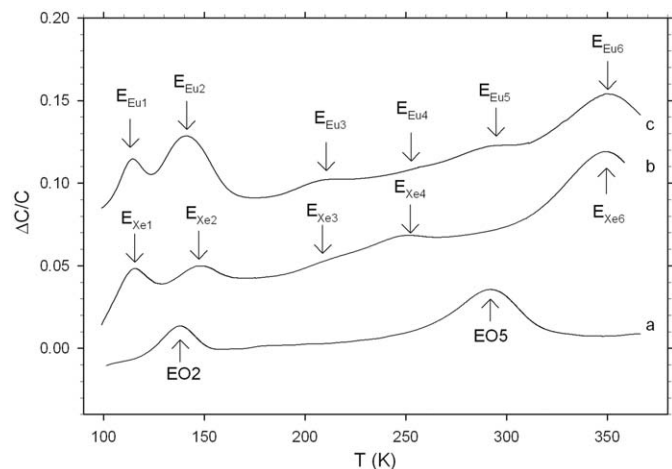


Fig. 1. DLTS spectra obtained for (a) GaN reference sample, (b) 1×10^{14} Eu cm⁻² implantation and (c) 1×10^{14} Xe cm⁻². Spectra were recorded using a reverse bias of -2 V, filling pulse of 2.2 V, pulse width of 2 ms and LIA frequency of 46 Hz (emission rate = 109 s⁻¹).

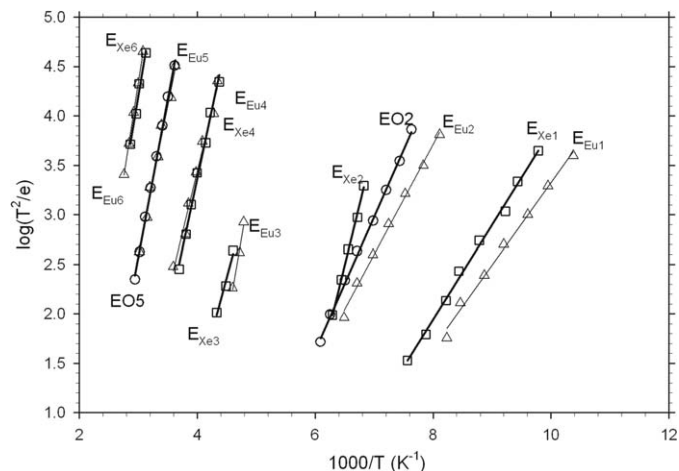


Fig. 2. Arrhenius plot showing defect signatures for all observed defect levels for the reference sample (circles), Eu implanted (triangles) and Xe implanted (squares) samples.

Table 1
Electronic properties of the defects introduced after Eu and Xe implantation in GaN.

Defect	$E_C - E_T$ (eV) $\pm 10\%$	σ (cm ⁻²) $\pm 10\%$	Identification	Reference
EO2	0.27	6.8×10^{-15}	EO2—Grown in defect	[8]
EO5	0.61	2.2×10^{-14}	EO5—V _N related	[8]
E _{Eu1}	0.19	2.6×10^{-16}	RE _{Ga} -V _N ?	[5,6]
E _{Eu2}	0.22	3.8×10^{-16}	Implantation related	–
E _{Eu3}	0.68	8.1×10^{-8}	Implantation related	–
E _{Eu4}	0.49	7.1×10^{-15}	E4—implantation related	[6]
E _{Eu5}	0.60	6.7×10^{-15}	EO5—Grown in defect	[8]
E _{Eu6}	0.77	5.2×10^{-14}	ER4—Implantation related	[9]
E _{Xe1}	0.19	1.2×10^{-15}	RE _{Ga} -V _N ?	[5,6]
E _{Xe2}	0.48	4.3×10^{-8}	Implantation related	–
E _{Xe3}	0.64	2.9×10^{-14}	Implantation related	–
E _{Xe4}	0.45	1.3×10^{-13}	E4—implantation related	[6]
E _{Xe6}	0.72	1.1×10^{-14}	ER4—Implantation related	[9]

section of 6.7×10^{-15} cm⁻². This defect level cannot be seen in the Xe implanted sample at all, most likely due to this peak appearing in the shoulder of the large broad peak at 340 K. The EO2 peak is also not observed in the Eu and Xe implanted spectra.

The general features of the two implanted spectra are qualitatively similar, although the peak positions are not all identical with the same defect signatures, possibly due to the above mentioned reasons. The defects labeled E_{Eu1} and E_{Xe1} both have the same energy level at $E_C - 0.19$ eV but the capture cross sections differ by almost an order of magnitude as 2.6×10^{-16} and 1.2×10^{-15} cm⁻², respectively. The same level has been observed by Song et al. after implantation with Er and Pr [6]. Density functional theory calculations done by Filhol et al. [5] considered the RE_{Ga}-V_N complex for the three rare-earth dopants (Eu, Er and Tm) in GaN, and showed that a half-filled level 0.2 eV below the conduction band is formed for all three RE ions. They showed that RE_{Ga} defects bind more strongly with V_N than any other species investigated, and that these pairs are stable to around 1000 °C. It has also been demonstrated that implanted RE ions generally occupy the substitutional Ga sites [7], which were the main motivation to consider the RE_{Ga}-V_N complex structure for calculations. Therefore the trap level at $E_C - 0.19$ eV in GaN could be attributed to RE_{Ga}-V_N. The fact that a similar level is observed after Xe implantation, indicates that this defect complex is not just RE related but has a more general structure where the implanted species might occupy the substitutional Ga position which can still bind with a mobile V_N forming a defect complex with the same electronic structure.

The defect labeled E_{Eu2} with activation energy of $E_C - 0.22$ eV might be related to the V_N according to Fang et al. [11] who observed this same defect as the main defect introduced during electron irradiation of GaN. The peak E_{Xe2} however, does not seem to be related to E_{Eu2} at all, since it results in a completely different level at $E_C - 0.48$ eV with a very large capture cross section of 4.2×10^{-8} cm⁻².

The defect peaks indicated by E_{Eu3} and E_{Xe3} were only clearly visible for the three lower rate window settings and could not be resolved from the spectra obtained using any of the higher rate window settings. The energy levels are $E_C - 0.68$ eV and $E_C - 0.64$ eV for the Eu and Xe implanted samples, respectively. A much larger value for the capture cross section for E_{Eu3} of 8.1×10^{-10} cm⁻² is obtained compared to 2.9×10^{-14} cm⁻² for E_{Xe3}. These two levels might be related, but due to only three points being used for the Arrhenius plot and the other factors, as mentioned above, result in less accurate values.

The close overlap of the defect signature lines for the defects labeled E_{Eu4} and E_{Xe4} as well as E_{Eu6} and E_{Xe6} might indicate that they are similar defects created during Eu and Xe implantation. Song et al. [6] also observed defect levels at $E_C - 0.60$ eV, $E_C - 0.41$ eV

for Er- and $E_C - 0.61$ eV, $E_C - 0.39$ eV for Pr-implanted GaN. The level at about $E_C - 0.40$ eV might be related to the $E_C - 0.49$ eV and $E_C - 0.45$ eV levels observed here for the E_{Eu4} and E_{Xe4} peaks, respectively, while the level at about $E_C - 0.60$ eV might be present in these samples as well, resulting in the broad peak around 290 K, which consists of a superposition with the $E_C - 0.62$ eV defect level already present in the material. Haase et al. [12] suggested that the level at around $E_C - 0.60$ eV is most likely due to the nitrogen antisite point defect, N_{Ga}. The defects E_{Eu4} and E_{Xe4} which might be similar to the $E_C - 0.40$ eV levels, cannot be related to RE dopant levels, as Song proposed, since the Xe implantation results in a similar level. This defect might therefore rather be some other implantation related defect complex being formed during the collision cascade.

In the work by Song, spectra were only measured up to 300 K, so they did not observe the peaks E_{Eu6} or E_{Xe6} at a temperatures around 350 K with activation energies $E_C - 0.77$ eV and $E_C - 0.72$ eV, respectively. Defect levels at $E_C - 0.77$ eV and $E_C - 0.95$ eV have also been observed after 5.4 MeV He irradiation in GaN [9]. This might also be similar to the E_{Eu6} or E_{Xe6} defects, although the $E_C - 0.95$ eV level is not present after Eu or Xe implantation.

4. Conclusion

In this work we report and compare the results of the electrical active defects of Eu- and Xe-implanted GaN samples. The high amount of radiation damage resulted in broadened and overlapping peaks in the DLTS spectra, complicating accurate defect identification. A defect level at $E_C - 0.19$ eV is observed which is also reported after Er- and Pr-implantation, originally associated with the RE_{Ga}-V_N complex. This defect cannot be related to the RE-complex alone, since this defect is also present after implantation with the inert ion Xe. It might be related to a more general implantation related defect complex. Other implantation related defect levels are also introduced with energy levels around $E_C - 0.22$ eV, $E_C - 0.68$ eV, $E_C - 0.49$ eV, $E_C - 0.60$ eV and $E_C - 0.77$ eV for Eu implantation and $E_C - 0.48$ eV, $E_C - 0.64$ eV, $E_C - 0.45$ eV and $E_C - 0.72$ eV for Xe implantation, of which at least two have been observed before introduced during ion implantation. Some of these levels have similar defect signatures and can be related to other RE implantation related defects.

Acknowledgements

V. Matias would like to acknowledge the financial assistance of the European Union under Contract no. HPRN-CT2001-00297 (RENI BEL), and the Fund for Scientific Research, Flanders (FWO)

contract G.0185.2. The group from UP also acknowledge the financial assistance of the National Research Foundation, South Africa.

References

- [1] S. Nakamura, G. Fasol, *The Blue Laser Diode*, Springer, Heidelberg, 1997.
- [2] P.N. Favennec, H. L'Haridon, M. Salvi, D. Moutonnet, Y. Le Guillou, *Electron. Lett.* 25 (1989) 718.
- [3] A.J. Steckl, H. Eikenfeld, D.S. Lee, M. Garter, *MSE B B81* (2001) 97.
- [4] H.J. Lozykowski, *Phys. Rev. B* 48 (24) (1993) 17758.
- [5] J.-S. Filhol, R. Jones, M.J. Shaw, P.R. Briddon, *Appl. Phys. Lett.* 84 (15) (2004) 2841.
- [6] S.F. Song, W.D. Chen, C. Zhang, L. Bian, C.C. Hsu, L.W. Lu, Y.H. Zhang, J. Zhu, *Appl. Phys. Lett.* 86 (2005) 2111.
- [7] B. Pipeleers, S.M. Hogg, A. Vantomme, *NIM B* 206 (2003) 95.
- [8] P. Hacke, T. Detchprohm, K. Hiramatsu, N. Sawaki, *J. Appl. Phys.* 76 (1994) 304.
- [9] F.D. Auret, S.A. Goodman, F.K. Koschnick, J.-M. Spaeth, B. Beaumont, P. Gibart, *Appl. Phys. Lett.* 74 (15) (1999) 2173.
- [10] D. Haase, M. Schmid, W. Kürner, A. Dörnen, V. Härle, F. Scholz, M. Burkard, H. Schweizer, *Appl. Phys. Lett.* 69 (17) (1996) 2525.
- [11] Z.Q. Fang, D.C. Look, W. Kim, Z. Fan, A. Botchkarev, H. Morkoc, *Appl. Phys. Lett.* 72 (1998) 2277.
- [12] D. Haase, M. Schmid, W. Kumer, A. Domen, V. Harle, F. Scholz, M. Burkard, H. Schweizer, *Appl. Phys. Lett.* 69 (1996) 2525.